Growth and characterization of straight InAs/GaAs nanowire heterostructures on Si substrate*

Yan Xin(颜 鑫), Zhang Xia (张 霞)†, Li Jun-Shuai(李军帅), Lü Xiao-Long(吕晓龙), Ren Xiao-Min(任晓敏), and Huang Yong-Qing(黄永清)

State Key Laboratory of Information Photonics and Optical Communications, Beijing University of Posts and Telecommunications, Beijing 100876, *China*

(Received 6 December 2012; revised manuscript received 6 March 2013)

Vertical InAs/GaAs nanowire (NW) heterostructures with a straight InAs segment have been successfully fabricated on Si (111) substrate by using AlGaAs/GaAs buffer layers coupled with a composition grading InGaAs segment. Both the GaAs and InAs segments are not limited by the misfit strain induced critical diameter. The low growth rate of InAs NWs is attributed to the AlGaAs/GaAs buffer layers which dramatically decrease the adatom diffusion contribution to the InAs NW growth. The crystal structure of InAs NW can be tuned from zincblende to wurtzite by controlling its diameter as well as the length of GaAs NWs. This work helps to open up a road for the integration of high-quality III-V NW heterostructures with Si.

Keywords: nanowire, Si, buffer layer, adatom diffusion

PACS: 61.46.Km **DOI:** 10.1088/1674-1056/22/7/076102

1. Introduction

III-V semiconductor materials have distinct advantages compared with Si, such as higher carrier mobilities, a direct bandgap and a wide range of bandgap engineering. Direct epitaxy of III-V semiconductors on Si substrate has been attracting a great deal of attention as it could allow the integration of III-V-based optoelectronics with established Si microelectronics.[1] However, achieving this integration requires overcoming several specific problems including lattice and thermal expansion mismatch, and the formation of antiphase domains.[2–4] Benefiting from a small lateral dimension, nanowires (NWs) can relieve the strain due to the lattice mismatch via lateral relaxation within the critical diameters.[5] However, since typical III-V NWs grow preferentially in the [111]B direction (or [111]A direction), while Si (111) surface has a nonpolar nature, three equivalent and tilted growth directions usually occur.[6]

In the previous work, we have successfully grown vertical and high-quality GaAs NWs on Si (111) substrate by using buffer layers.[7] To realize high-performance Si-based NW optoelectronic devices, high-quality Si-based NW heterostructures need to be fabricated. Up to now, two-dimensional (2D) $In_xGa_{1-x}As$/GaAs quantum-well heterostructures have been widely used in optoelectronic devices, especially in optical communication devices.[8] In comparison, one-dimensional InAs/GaAs heterostructures are still confronted with some difficulties. Due to the large lattice-mismatch, the critical diameter of the InAs segment in an InAs/GaAs axial NW heterostructure is rather small (about 44 nm).[5] In addition, a straight InAs-on-GaAs NW heterostructure is rather difficult to realize in Au-catalyzed growth as the Au/GaAs interfacial energy is lower than that of Au/InAs in most cases.[9,10] Most recently, Maria *et al.* has fabricated straight InAs-on-GaAs NW heterostructures under the condition that InAs exhibits a WZ structure, which is similar to the work reported by Hiruma *et al.* in 1996.[10,11] However, to fulfill the above requirement, some growth parameters, e.g., the NW diameter, the growth temperature, and the V/III ratio, should be controlled accurately.[12–15]

In this paper, we successfully fabricated straight InAs/GaAs nanowire heterostructures on Si substrate by using AlGaAs/GaAs buffer layers coupled with a composition grading InGaAs buffer segment. Both the GaAs NW and InAs NW are not limited by the misfit strain induced critical diameter. The crystal phase of InAs NW could be tuned from zincblende (ZB) to wurtzite (WZ) by controlling its diameter as well as the length of GaAs NWs. Other related phenomena are also discussed.

2. Experiment

The Au-assisted vapor-liquid-solid (VLS) growth was performed by using a Thomas Swan CCS-MOCVD system at a pressure of 1.33×10^4 Pa. Trimethylgallium (TMGa), trimethylaluminum (TMAl), trimethylindium (TMIn) and arsine were used as precursors. The carrier gas was hydrogen. The growth was carried out as the following steps: (i) the

*Project supported by the National Basic Research Program of China (Grant No. 2010CB327600), the National Natural Science Foundation of China (Grant Nos. 61020106007, 61077049, and 61211120195), the International Science and Technology Cooperation Program of China (Grant No. 2011DFR11010), the Specialized Research Fund for the Doctoral Program of Higher Education, China (Grant No. 20120005110011), the Programme of Introducing Talents of Discipline to Universities (111 Program) of China (Grant No. B07005), and the Excellent Ph. D. Students Foundation of Beijing University of Posts and Telecommunications, China (Grant No. CX201213).

†Corresponding author. E-mail: xzhang@bupt.edu.cn

© 2013 Chinese Physical Society and IOP Publishing Ltd

Si (111) substrate was chemically cleaned with a final treatment in HF/NH4F/H2O (1:5:6) solutions to remove the native oxide and form a hydrogen-terminated surface; (ii) the AlGaAs/GaAs buffer layers, which consisted of a 5-nm AlAs nucleation layer, a 15-nm $Al_{0.5}Ga_{0.5}As$ nucleation layer, and a 100-nm GaAs buffer layer, were grown on the Si substrate via a two-step growth;[16] (iii) an Au film with a thickness of 4 nm was deposited on the Si substrate by magnetron sputtering. Then the substrate was loaded into the MOCVD reactor and annealed *in situ* at 645 °C in arsine and hydrogen ambient; (iv) after ramped down to the desired temperature, GaAs NWs were grown via a two-temperature procedure consisting an initial growth at 510 °C for 10 s and a subsequential growth at 440 °C for a certain time;[7] (v) after raising the temperature to 470 °C, a composition grading InGaAs segment was grown for 200 s, during which the TMGa flow rate was decreased linearly from 4.1×10^{-5} mol·min^{-1} to 6×10^{-6} mol·min^{-1} and the TMIn flow rate was simultaneously increased linearly from 3.8×10^{-6} mol·min^{-1} to 3.4×10^{-5} mol·min^{-1}; (vi) with a TMIn flow rate of 3.4×10^{-5} mol·min^{-1}, growth of InAs NWs was initiated at 470 °C for 10 s and then proceeded at 400 °C for 500 s. The flow rate of AsH_3 was kept constant at 2.87×10^{-3} mol·min^{-1}. A schematic diagram of the NW heterostructure is shown in Fig. 1.

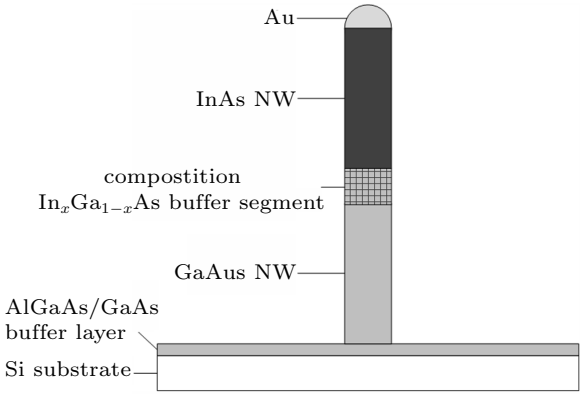


Fig. 1. Schematic diagram of the InAs/GaAs axial NW heterostructure on Si substrate.

In step (v), the growth time of GaAs NWs at 440 °C was set to 400 s, 200 s, and 50 s for sample A, B, and C, respectively. To investigate the influence of the AlGaAs/GaAs buffer layers as well as the InGaAs segment on the characteristics of the NWs, two samples were prepared as counterparts. Sample D without buffer layers was prepared by carrying out steps (i), (iii), (iv), (v), and (vi) Sample E without the composition grading InGaAs segment was prepared by carrying out steps (i), (ii), (iii), (iv), and (vi). Growth parameters of the five samples are listed in Table 1.

Morphologies of the samples were characterized by Field Emission Scanning Electron Microscopy (FESEM). Structural and compositional characteristics of the samples were investigated by Transmission Electron Microscopy (TEM) and Energy Dispersive Spectroscopy (EDS). TEM specimens were prepared by ultrasonicating the samples in ethanol for 5 min, followed by spreading drops from the suspension onto a holey carbon/Cu grid.

Table 1. Growth parameters of the five samples.

Sample	Buffer layers	GaAs NW	InGaAs segment	InAs NW
A	Yes	400 s	Yes	500 s
B	Yes	200 s	Yes	500 s
C	Yes	50 s	Yes	500 s
D	No	400 s	Yes	500 s
E	Yes	400 s	No	500 s

3. Results and discussion

Figures 2(a) and 2(b) show the SEM images of sample D. We can see that these NWs are random in growth direction and only a small proportion of them are vertical to the substrate. These orientations correspond to four ⟨111⟩ directions for a (111) oriented crystal with one orientation perpendicular to the surface and three orientations inclined to the substrate.[6] However, the single NW is straight along the growth direction as shown in the inset of Fig. 2(b). By growing AlGaAs/GaAs buffer layers on the Si substrate before NW growth, most of the NWs are vertical to the substrate as shown in Figs. 2(c) and 2(d). However, Au movement along with a downward or branched growth occurs on the upper part of most NWs, which has been commonly observed in the growth of axial InAs-on-GaAs NW heterostructures.[9,10] Figures 2(e) and 2(f) show the SEM images of sample A which was grown by using the buffer layers coupled with a composition grading InGaAs segment. We can see that over 80% of the NWs are perpendicular to the Si substrate. Most of the NWs are straight and without Au movement or downward/branched growth as shown in the inset of Fig. 2(f).

Comparing sample A with sample D and E, we can see the great contributions of AlGaAs/GaAs buffer layers and the composition grading InGaAs segment to the formation of vertical and the straight InAs/GaAs NW heterostructures on Si substrate. The high-quality buffer layers by a two-step process have be proved to be helpful to modifying the nonpolar nature of Si (111) surface which contributes to the vertical growth.[7] The composition grading InGaAs segment is critical to the formation of straight InAs NW on GaAs NW. Based on the theory proposed by Paladugu *et al.*, the interfacial energy between Au and GaAs is much smaller than that between Au and InAs. Thus, the Au particle would move sideways with further growth of InAs by preserving an interface with GaAs which results in a downward/branched growth of InAs.[9] By growing a composition grading InGaAs segment varying from GaAs to InAs before the growth of InAs NW, the large interfacial energy difference between Au/GaAs and Au/InAs is divided into many tiny ones between two adjacent $In_xGa_{1-x}As$ slices. As the upper slice can easily grow on the lower one due to a rather small interfacial energy difference, the InAs NW can certainly grow on the topmost $In_xGa_{1-x}As$ slice and the straight InAs-on-GaAs NW axial heterostructure is realized.

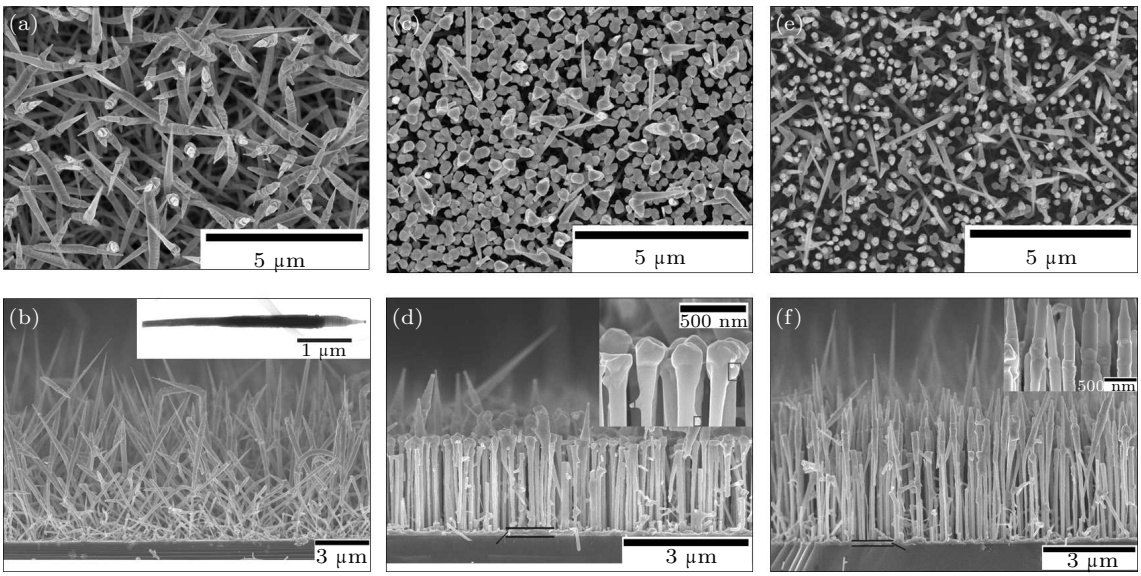


Fig. 2. SEM images of sample D, sample E, and sample A. (a), (c), and (e) show the top view SEM images of sample D, E, and A, respectively. (b), (d), and (f) show the cross sectional SEM images of sample D, E, and A, respectively. The inset in (b) shows the TEM image of a single NW from sample D. The insets in (d) and (f) show the amplified SEM image of the top parts of the NWs in (d) and (f), respectively. Rectangular frames in the inset in (d) indicate the dropping Au particles.

Figure 3 shows the TEM images of sample A and sample D. Figures 3(a) and 3(b) show the TEM images of the foot of a single NW from sample A. The NW exhibits a high quality and no threading dislocation or twins is observed. In contrast, a lot of threading dislocations and twins can be seen apparently in the NW from sample D, as is shown in Figs. 3(c) and 3(d). In addition, as reported by Chuang *et al.*, well-aligned GaAs NW can be grown on Si substrate if and only if its diameter is smaller than the critical diameter (about 100 nm), beyond which the lateral relaxation of the NW is not able to accommodate the misfit strain between GaAs NW and the Si substrate.[17] However, for sample A, an NW with a diameter of 110 nm grows successfully without defects as shown in Fig. 3(a). The high-quality and large-diameter NWs from sample A should be attributed to the AlGaAs/GaAs buffer layers as the misfit strain between GaAs and Si can be accommodated via generating dislocations in the buffer layers. Thus high-quality GaAs NWs can be grown epitaxially on the buffer layers without misfit strain.

Based on Glas's theory, there is a critical diameter (about 44 nm) in InAs/GaAs axial NW heterostructures caused by the misfit strain due to the large lattice mismatch between GaAs and InAs.[5] Beyond this value, dislocations and stacking faults will emerge in the InAs NW. This limitation can be solved by using the composition grading InGaAs segment. Figure 3(f) shows the InAs segment of a single NW from sample A. The InAs NW with a diameter of about 96 nm exhibits a high crystal quality without dislocations or stacking faults (detailed analyses of the crystal structure will be discussed later). It can be concluded that the composition grading InGaAs segment could effectively relieve the stress and strain resulting from the large lattice mismatch and reduce the total strain energy, thus the critical diameter increases remarkably. Besides, according to the latest report by Messing *et al.*, InAs NW can grow straightly on top of a GaAs NW only when the InAs segment has a WZ crystal structure.[10] However,

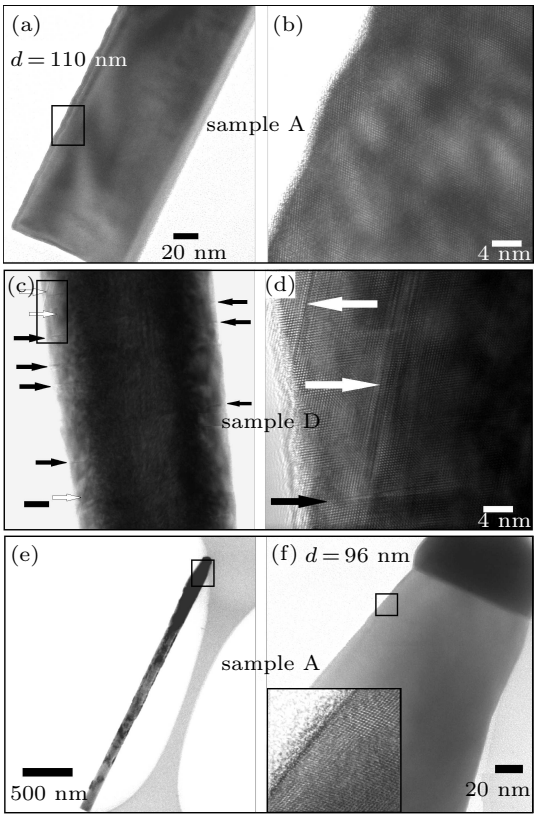


Fig. 3. TEM analyses of sample A and sample D. (a) and (b) show the foot of a single NW from sample A, (c) and (d) show the middle of a single NW from sample D, (e) and (f) show the InAs segment of a single NW from sample A. Threading dislocations and twins are indicated by black and white arrows, respectively. The inset in (f) shows the HRTEM of the top part of the InAs NW.

from the inset in Fig. 3(f), we can determine that the InAs NW here exhibits a pure ZB structure. This further supports our conclusion that the composition grading InGaAs segment can help to overcome the large interface energy difference between Au/GaAs and Au/InAs and lead to straight InAs NW on GaAs NW, independent of the crystal structure of InAs NW.

Figure 4 shows the SEM images of sample A, sample B, and sample C. GaAs, InGaAs, and InAs segments, which are determined by EDS line scans shown in Fig. 5, are indicated in the figures. The lengths of the GaAs segment are estimated to be 2.1 μm, 880 nm, and 200 nm, respectively, as estimated from the Scanning Transmission Electron Microscope (STEM) images in Fig. 5 (the actual length of the NWs is probably longer as NWs may be broken during ultrasonicating). The growth rates of the three samples are 5.3 nm/s, 4.4 nm/s, and 4 nm/s, respectively, which are comparable to those of GaAs NWs grown on Si substrate by using buffer layers while much lower than those on GaAs substrate.[7,18] The difference in the growth rate may be due to the different surface conditions between the AlGaAs/GaAs buffer layers grown on Si substrate and the GaAs substrate. The lengths of the InAs NWs from the three samples are estimated to be 850 nm, 1.15 μm, and 960 nm, which are much shorter than those on the GaAs NWs grown on GaAs substrate.[18] We believe that this is related to the special surface characteristics of buffer layers. It is well known that for VLS growth, there are two major contributions, i.e., direct impingement of the precursors onto the alloy droplet and adatom diffusion from the substrate surface and sidewalls to the top.[19,20] In this experiment, the lower growth rate of InAs NWs is probably due to the much lower contribution of adatom diffusion from the substrate surface. As reported by Kim *et al.*, the In diffusion length on the GaAs (111)B surface is limited to about 6 μm.[21] As shown in Fig. 4, the surface of AlGaAs/GaAs buffer layers is uneven and full of bumps and holes, which means that the surface area is much larger than the smooth GaAs surface and the corresponding surface distance between two certain points is much longer. Thus the In adatoms could be consumed more sufficiently at the same length and much less adatoms can reach the Au particle. In addition, it has been demonstrated that In adatoms preferentially incorporate onto those concave areas constructed by high-index surfaces of the GaAs NW sidewalls to minimize the local surface energy.[22] This conclusion also applies equally here, since the top of the buffer layers is a layer of GaAs which contains a lot of concave regions for In adatoms' adhesion. Based on the two mechanisms aforementioned, it can be concluded that the coarse and rugged AlGaAs/GaAs buffer layers act as a reservoir for In adatoms, which decrease the adatom diffusion contribution to the InAs NW growth.

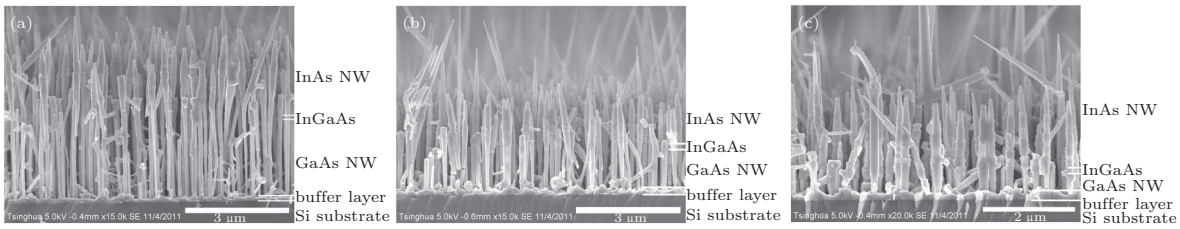


Fig. 4. SEM images of (a) sample A, (b) sample B, and (c) sample C.

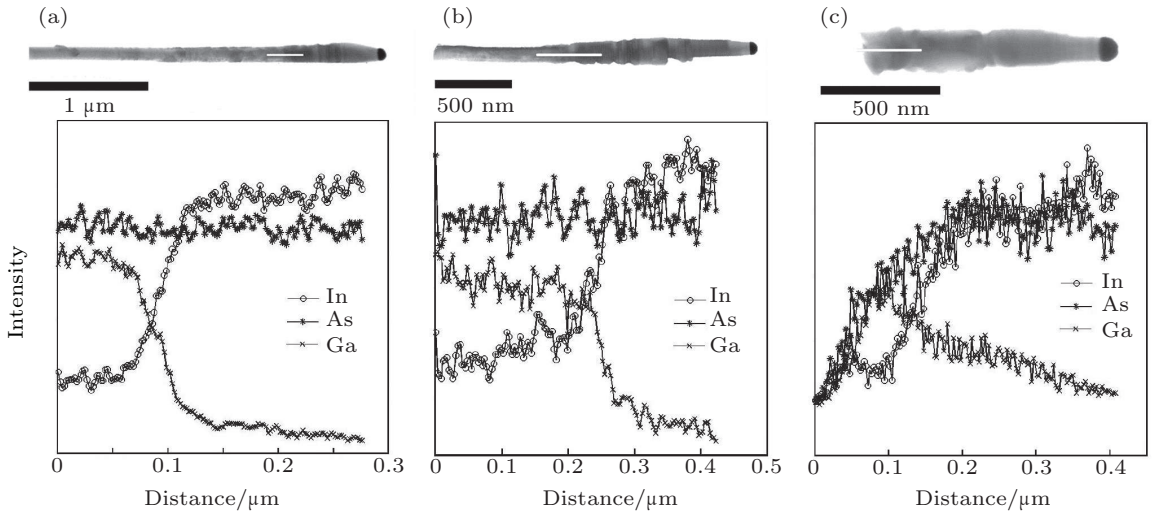


Fig. 5. EDS analyses of a single NW from (a) sample A, (b) sample B, and (c) sample C. The grey rectangular area in every image indicates the InGaAs segment.

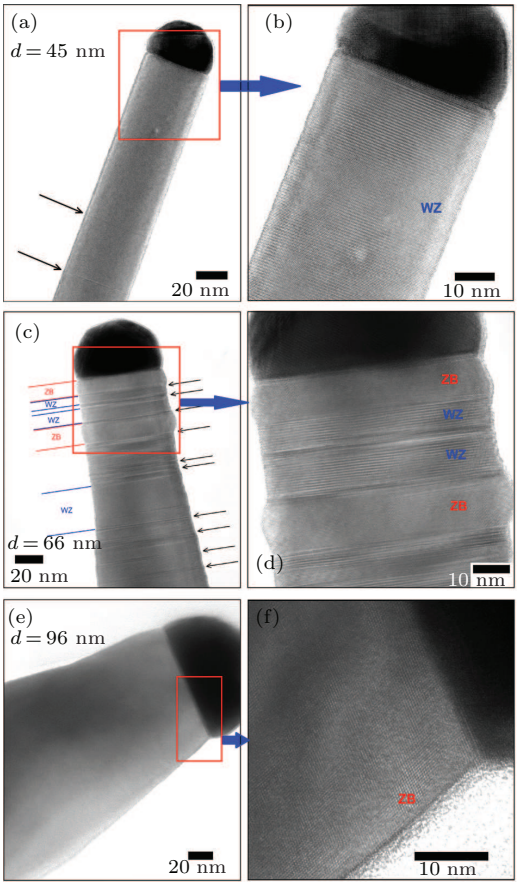


Fig. 6. (color online) TEM analyses of InAs NWs with different diameters from sample A. (a) and (b) show a single NW with a diameter of 45 nm, (c) and (d) show a single NW of 66 nm, (e) and (f) show a single NW of 96 nm. Stacking faults are indicated by black arrows.

Figure 6 shows the TEM images of InAs NWs with different diameters from sample A. For the thinnest one with a diameter of 45 nm (Fig. 6(a)), the structure is a WZ with very little stacking faults. Increasing the diameter to 66 nm (Fig. 6(b)), the structure is composed of a mixture of ZB and WZ phases and a lot of stacking faults can be observed. Finally, for the thickest one with a diameter of 96 nm, the NW exhibits a pure ZB structure with nearly no stacking faults or other defects. The dependence of crystal structure of InAs NW on diameter was also observed by other groups.[12–14] As discussed by Shtrikman *et al.*, for GaAs and InAs NWs, the free energy of the wire is lower for WZ than for ZB, thus, the WZ phases occur during growth. However, when the diameter increases, the inside volume cohesive energy, which is lower for ZB than for WZ, becomes dominant thus stacking faults and ZB segments are likely to form.[22] Figure 7 shows the TEM images of InAs NWs from sample B and C. For the NW with a diameter of 76 nm from sample B (Fig. 7(a)), the structure is mainly a WZ with dense stacking faults. While for a much thicker NW (the diameter is about 93 nm) from sample B (Fig. 7(b)), the structure is also a WZ but the density of stacking faults is much lower than that in Fig. 7(a). Comparing the structure characteristics of InAs NWs among sample A, B, and C, we can conclude that the crystal phase of InAs NW is also influenced by the length of the nether GaAs NW. At a large diameter, the NW exhibits a phase transition from the pure ZB to mainly WZ with the decrease of the length of GaAs NW. This phenomenon has been discussed in our previous work that the GaAs NWs with different lengths could control the adatom diffusion contribution, especially the adatom diffusion from the sidewalls to the top, which further affects the crystal phase of InAs NW.[18]

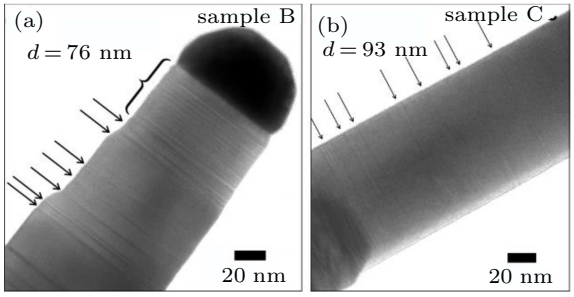


Fig. 7. TEM analyses of NWs from (a) sample B and (b) sample C. Stacking faults are indicated by black arrows.

4. Conclusions

In conclusion, we have successfully fabricated straight InAs/GaAs NW heterostructures on Si substrate by using AlGaAs/GaAs buffer layers coupled with a composition grading InGaAs segment. The GaAs NWs exhibiting high crystal quality as the misfit strain between GaAs and Si can be accommodated via generating dislocations in the buffer layers. Both the GaAs and InAs segments are not limited by the misfit strain induced critical diameter. The low growth rate of InAs NW is attributed to the rugged AlGaAs/GaAs buffer layers which dramatically decrease the adatom diffusion contributed to the InAs NW growth. We also demonstrate that the crystal structure of InAs NW could be tuned by controlling its diameter as well as the lengths of GaAs NWs. This work helps to open new possibilities for the integration of high-quality III-V NW heterostructures on Si substrate.

References

[1] Yeh H J J and Smith J S 1994 *IEEE Photon. Technol. Lett.* **6** 706
[2] Fang S F, Adomi K, Iyer S, Morkoc H, Zabel H, Choi C and Otsuka N 1990 *J. Appl. Phys.* **68** R31
[3] Ishiwara H, Hoshino T and Katahama H 1995 *Mater. Chem. Phys.* **40** 225
[4] Komninou P, Stoemenos J, Dimitrakopulos G P and Karakostas T 1994 *J. Appl. Phys.* **75** 143
[5] Glas F 2006 *Phys. Rev. B* **74** 121302
[6] Roest A L, Verheijen M A, Wunnicke O, Serafin S, Wondergem H and Bakkers E P A M 2006 *Nanotechnology* **17** S271
[7] Huang H, Ren X M, Ye X, Guo J W, Wang Q, Yang Y S, Cai S W and Huang Y Q 2010 *Nano Lett.* **10** 64
[8] Takeuchi T, Chang Y L, Tandon A, Bour D, Corzine S, Twist R, Tan M and Luan H C 2002 *Appl. Phys. Lett.* **80** 2445
[9] Paladugu M, Zou J, Guo Y N, Auchterlonie G J, Joyce H J, Gao Q, Tan H H, Jagadish C and Kim Y 2007 *Small* **3** 1873
[10] Messing M E, Wong J, Zanolli Z, Joyce H J, Tan H H, Gao Q, Wallenberg L R, Johansson J and Jagadish C 2011 *Nano Lett.* **11** 3899

[11] Hiruma K, Murakoshi H, Yazawa M and Katsuyama T 1996 *J. Cryst. Growth* **163** 226

[12] Caroff P, Dick K A, Johansson J, Messing M E, Deppert K and Samuelson L 2009 *Nat. Nanotechnol.* **4** 50

[13] Johansson J, Dick K A, Caroff P, Messing M E, Bolinsson J, Deppert K and Samuelson L 2010 *J. Phys. Chem. C* **114** 3837

[14] Shtrikman H, Popovitz R, Kretinin A, Houben L, Heiblum M, BukałM, Galicka M, Buczko R and Kacman P 2009 *Nano Lett.* **9** 1506

[15] Joyce H J, Wong J, Gao Q, Tan H H and Jagadish C 2010 *Nano Lett.* **10** 908

[16] Huang H, Ren X M, Lv J H, Wang Q, Song H L, Cai S W, Huang Y Q and Qu B 2008 *J. Appl. Phys.* **104** 113114

[17] Cirlin G E, Dubrovskii V G, Soshnikov I P, Sibirev N V, Samsonenko Y B, Bouravleuv A D, Harmand J C and Glas F 2009 *Phys. Status Solidi RRL* **3** 112

[18] Huang H, Ren X M, Ye X, Guo J W, Wang Q, Zhang X, Cai S W and Huang Y Q 2010 *Nanotechnology* **21** 475602

[19] Wagner R S and Ellis W C 1964 *Appl. Phys. Lett.* **4** 89

[20] Dubrovskii V G, Sibirev N V, Cirlin G E, Soshnikov I P, Chen W H, Larde R, Cadel E, Pareige P, Xu T, Grandidier B, Nys J P, Stievenard D, Moewe M, Chuang L C and Chang C 2009 *Phys. Rev. B* **79** 205316

[21] Kim Y, Joyce H J, Gao Q, Tan H H, Jagadish C, Paladugu M, Zou J and Suvorova A A 2006 *Nano Lett.* **6** 599

[22] Paladugu M, Zou J, Guo Y N, Zhang X, Joyce H J, Gao Q, Tan H H, Jagadish C and Kim Y 2009 *Angew. Chem. Int. Ed.* **48** 780